

000 PEVLM: PARALLEL ENCODING FOR VISION- 001 002 LANGUAGE MODELS 003 004

005 **Anonymous authors**

006 Paper under double-blind review

007 008 ABSTRACT 009

010 Vision-Language Models (VLMs) have demonstrated strong capabilities in
011 multimodal understanding and generation tasks. However, their application to long
012 video understanding remains hindered by the quadratic complexity of standard
013 attention mechanisms. In this work, we introduce **PEVLM**, a fine-tuning-free
014 parallel encoding method designed to enhance the prefilling efficiency of VLMs in
015 long video scenarios. To the best of our knowledge, this is the first work to adapt
016 parallel encoding to VLMs. PEVLM partitions the input video into context blocks
017 with a shared sink block, while preserving sequential position embeddings to align
018 the attention score distribution with that of Full-Attention. This design reduces the
019 complexity of attention from $O((T \times N)^2)$ to $O(T \times N)$ where T is the number
020 of frames and N the number of tokens per frame, with minimal loss in accuracy.
021 Extensive experiments across multiple state-of-the-art models and benchmarks
022 demonstrate that PEVLM consistently outperforms existing parallel encoding
023 approaches, achieving up to **7.47x** speedup in attention computation and reducing
024 end-to-end latency by **44%** to **50%**. Remarkably, PEVLM not only maintains high
025 accuracy, but in some settings even surpasses Full-Attention performance. Under
026 strict latency constraints, it achieves substantial gains, improving accuracy from
027 **23.26%** to **61.03%**. These results underscore the effectiveness of PEVLM for
028 low-latency, long-context video understanding, making it a promising solution for
029 real-world applications.

030 031 1 INTRODUCTION

032 In recent years, Vision-Language Models (VLMs) have become a central research focus at the
033 intersection of computer vision and natural language processing. These models have demonstrated
034 impressive performance in a wide range of multimodal understanding and generation tasks (Alayrac
035 et al., 2022; Li et al., 2020; Zhang et al., 2024c; Chen et al., 2024; Bai et al., 2025). As their
036 capabilities continue to improve, VLMs are being applied in increasingly complex domains, including
037 robotics (Black et al., 2024; Luo et al., 2025; Team et al., 2025), autonomous driving (Gao et al., 2024;
038 Hu et al., 2023; Wang et al., 2024), and healthcare (Liu et al., 2024). These application scenarios
039 often demand processing longer video inputs.

040 However, a key obstacle to applying VLMs to long-video inputs is the quadratic complexity of
041 transformer attention during the prefilling stage (Vaswani et al., 2017; Beltagy et al., 2020). To
042 address this issue, a widely adopted technique in large language models (LLMs) is the parallel
043 encoding mechanism (Li et al., 2024b; Acharya et al., 2025; Ma et al., 2025; Ratner et al., 2023;
044 Yang et al., 2025; Yen et al., 2024; Lu et al., 2024). In this approach, the input context is divided into
045 multiple blocks, each block independently encoded into Key-Value (KV) states, thus reducing the
046 computational complexity from $O(L^2)$ to $O(L)$. Moreover, parallel encoding alleviates the issue
047 of “lost in the middle phenomenon” by reducing the number of tokens participating in the softmax
048 operation and can even achieve accuracy surpassing that of Full-Attention in some scenarios (Liu
049 et al., 2023; Yang et al., 2025; Veličković et al., 2025).

050 Given this context, a natural question arises: Can existing parallel encoding methods for LLMs
051 be directly applied to VLMs for faster inference and deployment? In Table 1, we evaluate several
052 state-of-the-art models on widely used video benchmarks. Although we observe significant accuracy
053 drops with these methods, especially for models in the Qwen-VL family and the InternVL3_5 family.

054 In extreme cases, the output becomes empty or garbled, with accuracy falling to 0%. To investigate
 055 this, we analyze attention score distributions and find a misalignment between Full-Attention and
 056 parallel encoding. Based on this insight, we propose PEVLM (Parallel Encoding for Vision-Language
 057 Models—a new attention mechanism tailored for VLMs). PEVLM requires no fine-tuning, introduces
 058 no additional parameters, and involves minimal code changes, making it a lightweight solution to
 059 accelerate long-video processing in both cloud and edge settings. Our contributions are as follows.
 060

- 061 • We systematically analyze the distribution characteristics of attention scores under parallel
 062 encoding in VLMs, identifying a key reason for the misalignment between the attention
 063 score distributions of parallel encoding and Full-Attention: reusing position embeddings
 064 across blocks leads to the loss of critical video information.
- 065 • We propose PEVLM to recover the accuracy of parallel encoding by applying three alignment
 066 steps: (i) segmenting contexts into blocks by video frames rather than tokens; (ii) using the
 067 system prompts and the initial frames of the video as Sink Block for all blocks to avoid the
 068 duplication of abnormal distribution of initial tokens; (iii) preserving the sequential position
 069 embeddings instead of reusing position embeddings across blocks. With these alignment
 070 strategies, PEVLM reaches higher accuracy than existing parallel encoding methods, and
 071 reaches 98.24% to 104.80% of the accuracy of Full-Attention on different models.
- 072 • PEVLM reduces the computational complexity of the attention mechanism from $O((T \times N)^2)$ to $O(T \times N)$, where T is the number of frames and N the number of tokens per frame.
 073 (i) For 100k (text&video) token contexts prefilling, the attention layer achieves a 7.47x
 074 speedup, while the end-to-end 2.58x speedup without compromising generation quality. This
 075 highlights the practical viability and superiority of PEVLM in cloud deployment scenarios.
 076 (ii) Under fixed latency constraints, PEVLM increases accuracy from 23.26% to 61.03%,
 077 showcasing its critical value for latency sensitive applications.

078 2 OBSERVATIONS

081 To appropriately adapt the parallel encoding method for VLMs, in this section, we first review the
 082 foundational components of the standard attention mechanism, and then highlight the key differences
 083 between its application in LLMs and VLMs. These differences explain why off-the-shelf LLM
 084 parallel encoding methods underperform in long-video VLMs, motivating the design of PEVLM.

085 2.1 STANDARD ATTENTION MECHANISM

087 The softmax attention mechanism (Vaswani et al., 2017) serves as the core of transformer-based
 088 models. For a given query $Q \in \mathbb{R}^{n \times d}$, keys $K \in \mathbb{R}^{m \times d}$, and values $V \in \mathbb{R}^{m \times d}$, the output is
 089 computed as:

$$090 \quad O = \text{Softmax} \left(\frac{QK^T}{\sqrt{d}} \right) V, \quad (1)$$

092 where d is the model dimension.

094 Two key phenomena influence attention behavior in long sequences. First, the attention sink
 095 effect (Lab & AI, 2023; Sun et al., 2024) causes tokens at the input’s beginning, often the BOS
 096 token or system prompt, to consistently receive disproportionately high attention scores, anchoring
 097 the model’s focus. Second, position embeddings encode token order, enabling the model to discern
 098 sequential relationships. During prefilling, the computational cost is $OP_{\text{Attn}} = 2HL^2$, yielding $O(L^2)$
 099 complexity, where L is the context length and H the hidden size. This quadratic scaling severely
 100 bottlenecks inference for long inputs like extended videos.

101 2.2 KEY DIFFERENCES: LLMs vs. VLMs

103 **Attention Sink** APE (Yang et al., 2025) and Star-Attention (Acharya et al., 2025) have shown that
 104 sharing a common attention sink across parallel encoding blocks significantly enhances the accuracy
 105 of LLMs. **However, it has been observed that attention sinks are present not only in the initial**
 106 **system prompt, but also in the video frames in VLMs** (Huang et al., 2024; Zhang et al., 2024b;
 107 Kang et al., 2025). Drawing on the experience of applying attention sinks in LLMs, achieving optimal
 108 performance in VLMs may require incorporating a sufficient number of frames into the sink.

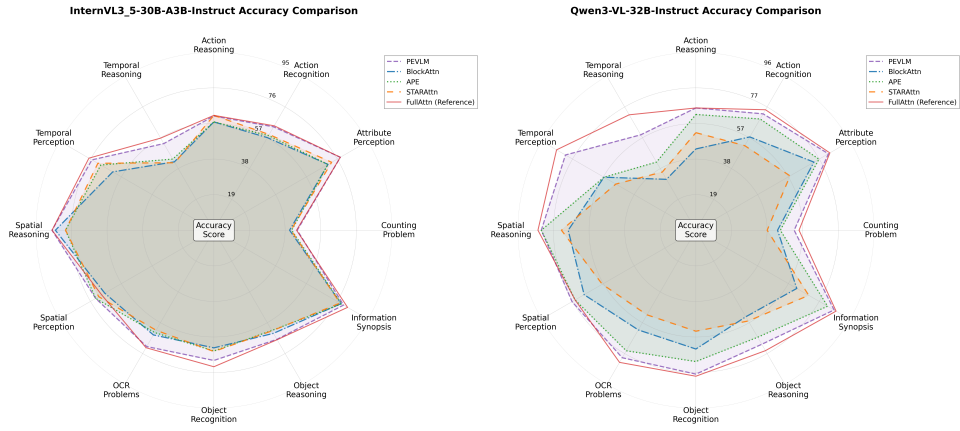
108
109
110
111
112
113
114
115
116
117
118
119
120
121

Figure 1: Radar-chart comparison of attention mechanisms (Full Attention, PEVLM, APE, BlockAttn, and StarAttn) on two representative large-scale models: InternVL3.5-30B-A3B (left) and Qwen3-VL-32B (right). PEVLM closely matches Full Attention across all Video-MME categories, while other methods (APE, BlockAttn, StarAttn) show noticeable degradation. More detailed results for all model scales are provided in Appendix G.

Position Embedding Recent efficient attention mechanisms, such as APE (Yang et al., 2025), Block Attention (Ma et al., 2025), and Star Attention (Acharya et al., 2025), often rely on reusing or sharing position embeddings across blocks to support parallel prefilling. However, these designs introduce significant limitations in video-centric tasks. In temporally sensitive categories and OCR-related tasks that require fine-grained spatial alignment across frames, these methods exhibit clear accuracy degradation compared to Full Attention (as shown in Figure 1). We find that the major performance drop arises from the reuse of position embeddings: compressing heterogeneous frame sequences into repeated positional templates disrupts the temporal identity of each frame, weakens cross-frame alignment, and distorts long-range dependency modeling.

So, preserving the correct temporal order of video frames is critical for video understanding tasks. Blindly reusing position embeddings across blocks can disrupt the model’s ability to capture temporal dependencies.

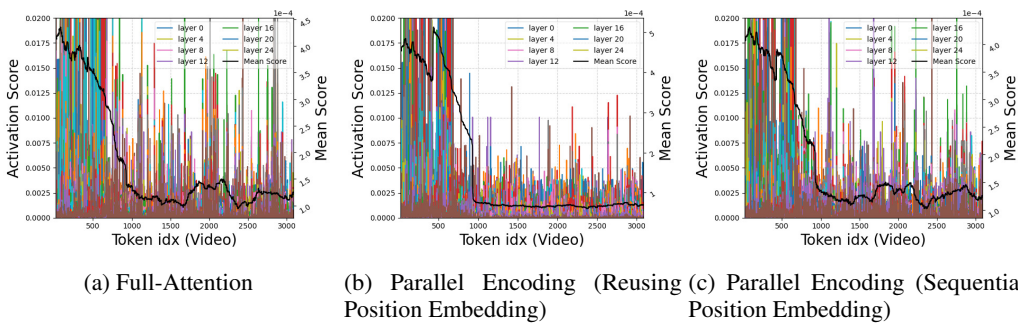
140
141
142
143
144
145
146
147
148
149
150

Figure 2: We examine the distributions of attention scores under Full Attention and Parallel Encoding using different positional embedding strategies, and further compute their moving averages (referred to as the mean score) to enable more systematic comparison. Due to space constraints, we present only the results on Qwen2.5-VL, more results are provided in Appendix H.

151
152
153
154
155
156
157
158
159
160
161

To support the above observations, we further collect the distribution of attention scores under Full-Attention and Parallel Encoding with different position embedding strategies, as shown in Figure 2, and summarize two key findings: (i) As shown in Figure 2(a), attention sinks are present not only in the initial system prompt, but also in the early video frames in VLMs. This suggests that it should be necessary to include early video frames when selecting sink tokens. (ii) As shown in Figure 2(b), compared to Full-Attention, the initial video frames receive even higher attention scores, while the remaining frames exhibit more uniform and lower attention scores. In contrast, when sequential

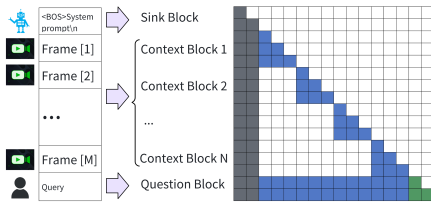
162 position embeddings are preserved, as illustrated in Figure 2(c), parallel encoding yields an attention
 163 score distribution that more closely resembles that of Full-Attention. These findings underscore the
 164 need for a VLM-specific parallel encoding strategy, which we introduce in the next section.
 165

166 3 PEVLM

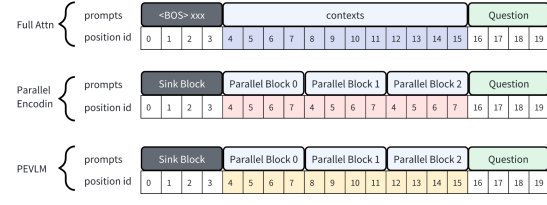
167 With the observations in the last section, we design PEVLM, which adaptively aligns the distribution
 168 of attention scores between Full-Attention and parallel encoding in VLMs, thereby boosting efficiency
 169 and performance.
 170

171 3.1 PARTITIONING STRATEGY

172 As illustrated in Figure 3a, PEVLM partitioning strategy consists of three core steps:
 173



174 (a) The PEVLM Masks.
 175



176 (b) Position Encoding in PEVLM
 177

178 Figure 3: Illustration of Position Encoding and Masks in PEVLM
 179

180 **Sink Block:** The initial text tokens (e.g., BOS token and system prompts) and the first several video
 181 frames are grouped into a dedicated Sink Block.
 182

183 **Context Blocks:** The remaining video content is uniformly partitioned into Context Blocks by frames
 184 to reduce computational overhead and enable parallelization.
 185

186 **Question Block:** The text tokens that follow the video input are left unsegmented as Question Block.
 187

188 As described in the *Observations* section, similar to the case in LLMs, applying parallel encoding
 189 methods in VLMs suffers from the misalignment of attention score distributions when compared
 190 to Full-Attention. While prior work has attempted to address this issue by introducing additional
 191 hyperparameters to realign attention scores (Yang et al., 2025), such approaches are not ideal for
 192 efficient deployment. To address this, PEVLM draws inspiration from Block Attention (Ma et al.,
 193 2025) and TurboRAG (Lu et al., 2024), and retains sequential position embeddings, as shown in
 194 Figure 3b. In contrast to these methods, which dynamically adjust positional embeddings, often to
 195 accommodate context reuse through sequence reordering, PEVLM forgoes such updates. Since video
 196 frames are processed in their original temporal order, PEVLM directly applies the sequential position
 197 embedding to each visual token within context blocks, without modifying their positions after query
 198 concatenation.
 199

200 By preserving sequential position embeddings, PEVLM maintains attention score distributions that
 201 closely resemble those of Full-Attention. It is worth noting that, unlike some parallel encoding
 202 methods in LLMs that can enhance a model’s ability to process longer contexts (Ratner et al.,
 203 2023; Yang et al., 2025), PEVLM does not provide such benefits. Because PEVLM preserves the
 204 original positional embedding of every input token, unlike in LLMs, it cannot effectively extend
 205 a model’s usable context length. For example, in the case of LongVILA-7B-256f, the optimal
 206 number of sampled frames is 256. Using a higher frame sampling rate does not improve the model’s
 207 accuracy. For PEVLM, higher sampling rates (which correspond to longer sequence lengths) can yield
 208 better acceleration ratios; however, PEVLM does not improve model accuracy once the sampling
 209 rate exceeds the optimal 256-frame setting. Therefore, all subsequent accuracy and performance
 210 evaluations in following sections are conducted within each model’s optimal frame sampling range.
 211 Although increasing the sampling frequency may superficially provide larger speedup, it brings no
 212 accuracy benefits and is thus unnecessary.
 213

216 3.2 FORMULATIONS
217218 The computational formulation of PEVLM is defined as:
219

220
$$\text{Attn}_s = f(Q_s, K_s, V_s), \quad (2)$$

221

222
$$\text{Attn}_{c_i} = f(Q_{c_i}, K_{s+c_0+\dots+c_{i-1}}, V_{s+c_0+\dots+c_{i-1}}), \quad (3)$$

223

224
$$\text{Attn}_q = f(Q_q, K_{s+c_{\text{all}}+q}, V_{s+c_{\text{all}}+q}), \quad (4)$$

225

226 where s denotes the Sink Block, q denotes the Question Block, and c_i denotes the i -th Context Block.
227 Symbols Attn_s , Attn_{c_i} , and Attn_q represent the attention outputs for the corresponding blocks. The
228 function $f(\cdot)$ corresponds to the standard softmax attention defined in Equation (1), with Q , K and
229 V denoting the query, key, and value matrices respectively.
230231 The total computational operation (OP) count of PEVLM is:
232

233
$$\text{OP}_{\text{PEVLM}} = \text{OP}_{\text{Sink}} + N \times \text{OP}_{\text{ContextBlock}} + \text{OP}_{\text{Quest}}, \quad (5)$$

234

235
$$\text{OP}_{\text{Sink}} = 2HS^2, \quad (6)$$

236

237
$$\text{OP}_{\text{ContextBlock}} = 2HB(S + B), \quad (7)$$

238

239
$$\text{OP}_{\text{Quest}} = 2HQL, \quad (8)$$

240

241 where S denotes the sink block size, N denotes the context block number, B denotes the context
242 block size, Q denotes the query block size and H is the hidden size. L is the total token number and
243 $L = S + N \times B + Q$.
244245 After simplification:
246

247
$$\text{OP}_{\text{PEVLM}} = 2H(S^2 + Q^2 + NB^2 + QS + NQB + NSB). \quad (9)$$

248

249 As S , B , and Q are fixed, both L and OP_{PEVLM} are linearly proportional to N , and therefore the
250 computational complexity of PEVLM is $O(L)$. Compared to the $O(L^2)$ complexity of Full-Attention,
251 PEVLM significantly reduces the computational load of the attention mechanism.
252253 3.3 SINK&CONTEXT BLOCK SIZES
254255 Since the information within each video frame represents spatial content at a specific moment,
256 while information across frames reflects temporal dynamics, videos naturally possess structural
257 boundaries. If the video is divided into sink and context blocks by token count, this may to some
258 extent compromise the spatial integrity of the boundary frames shared between adjacent blocks. So
259 we divide the video by frame.
260261 As analyzed in the previous section, the number of frames selected for the Sink Block depends
262 primarily on the distribution of attention scores. The optimal strategy is to include all tokens with
263 significantly higher attention scores at the beginning of the video in the Sink Block. However, on the
264 one hand, the number of frames containing visual tokens with a high attention score varies across
265 different videos; on the other hand, as shown in Equation 9, a larger sink block size leads to higher
266 latency, resulting in a trade-off between accuracy and efficiency. A similar trade-off also exists in
267 determining the context block size. We will further analyze this in Section 5.
268269 4 EXPERIMENTS
270271 In this section, we test PEVLM from multiple perspectives against several different VLMs. The
272 primary objective is to evaluate the accuracy, computational efficiency, and real-world applicability of
273 PEVLM for long-video processing. And to better reflect practical deployment scenarios, we designed
274 the experiments from two perspectives. (i) We first test with workloads of approximately 100k tokens
275 to assess the acceleration performance of PEVLM in cloud serving platforms. (ii) Furthermore,
276 we evaluate PEVLM on the LongVideoBench dataset under a given latency constraint, in order to
277 measure its effectiveness in edge scenarios where both computational resources and latency are
278 limited.
279280 4.1 ACCURACY EVALUATION
281282 This experiment aims to evaluate the impact of PEVLM on accuracy in long-video understanding
283 tasks.
284

270 Table 1: Performance (\uparrow) of different models and different methods on video understanding tasks
 271 evaluated at tokens from 26k to 100k.

Method	MVBench 17s avg.	EgoSchema 3mins avg.	VideoMME < 2mins	VideoMME 2mins-1h	LongVideoBench (Val) < 1min	LongVideoBench (Val) 1min-1h	Avg.
InternVL3_5-30B-A3B-Instruct							
Full Attn	75.33%	83.60%	77.67%	63.94%	74.52%	58.81%	72.31%
Block Attn (ICLR25)	64.33%	79.60%	69.89%	58.17%	65.37%	54.61%	65.33%
APE (ICLR25)	64.81%	79.60%	71.22%	58.11%	67.31%	53.59%	65.77%
Star Attn (ICML25)	70.44%	79.80%	70.67%	58.89%	69.53%	53.59%	67.15%
PEVLM	73.53%	83.00%	77.00%	62.67%	73.41%	58.40%	71.34%
Qwen3-VL-8B-Instruct							
Full Attn	69.36%	73.00%	80.33%	68.00%	77.29%	63.52%	71.92%
Block Attn (ICLR25)	67.92%	65.80%	68.56%	54.00%	71.75%	50.31%	63.06%
APE (ICLR25)	64.22%	69.60%	65.11%	56.56%	68.70%	56.45%	63.44%
Star Attn (ICML25)	58.58%	12.40%	12.89%	60.56%	51.25%	58.71%	42.40%
PEVLM	69.42%	71.40%	80.11%	64.17%	76.73%	62.09%	70.65%
Qwen2.5-VL-7B-Instruct							
Full Attn	68.47%	57.00%	74.56%	56.72%	72.85%	55.33%	64.16%
Block Attn (ICLR25)	66.03%	47.40%	65.22%	50.39%	70.64%	47.85%	57.92%
APE (ICLR25)	66.03%	57.20%	50.56%	1.06%	54.02%	3.38%	38.71%
Star Attn (ICML25)	60.19%	19.80%	3.00%	0.00%	49.03%	0.00%	22.00%
PEVLM	68.44%	61.00%	74.33%	58.83%	74.52%	57.58%	65.78%
LongVILA-7B-256f							
Full Attn	61.92%	57.00%	66.33%	49.39%	65.10%	47.44%	57.86%
Block Attn (ICLR25)	57.81%	59.00%	64.89%	51.44%	61.77%	48.05%	57.16%
APE (ICLR25)	60.00%	60.60%	68.56%	51.61%	63.71%	46.93%	58.57%
Star Attn (ICML25)	63.39%	61.60%	70.11%	54.17%	63.43%	47.44%	60.02%
PEVLM	63.53%	61.40%	69.44%	54.33%	65.93%	49.18%	60.64%
LLaVA-Video-7B-Qwen2							
Full Attn	60.67%	58.20%	75.33%	59.99%	72.02%	55.53%	63.62%
Block Attn (ICLR25)	56.86%	51.60%	67.56%	55.50%	63.99%	52.36%	57.98%
APE (ICLR25)	58.00%	57.60%	72.22%	58.19%	67.87%	54.61%	61.42%
Star Attn (ICML25)	59.31%	57.80%	72.89%	58.71%	68.98%	54.92%	62.10%
PEVLM	60.00%	58.20%	74.33%	59.99%	72.02%	55.53%	63.35%

4.1.1 SETUP

We adopt LongVideoBench (Zhang & Wang, 2024), VideoMME (Fu et al., 2024), EgoSchema (Mangalam et al., 2023), MVBench (Li et al., 2024a) and MME-VideoOCR (Shi et al., 2025) as benchmarks, which are designed to comprehensively evaluate multimodal models in video understanding. All evaluations are conducted using the lmms-eval toolkit (Zhang et al., 2025b). We test on LLaVA-Video (Zhang et al., 2024c), LongVILA (Chen et al., 2024), Qwen2.5-VL (Bai et al., 2025), Qwen3-VL (Team, 2025) and InternVL3_5 (Wang et al., 2025a) as representative models. To minimize accuracy loss, all experiments are conducted with bf16 precision.

We compared the accuracy of Full-Attention, Block-Attention, APE, Star-Attention, and PEVLM in the datasets. Since the other methods are fine-tuning-free, we did not fine-tune the weights in the Block Attention test. For APE, we conducted experiments with a temperature setting of $T = 1.0$. This choice was motivated by two considerations. First, lowering the temperature further leads to additional accuracy degradation. As previously observed, parallel encoding tends to produce lower attention score distributions over context blocks in VLMs, rather than higher. Therefore, decreasing the temperature further skews the attention distribution away from that of Full-Attention, exacerbating the accuracy loss. Second, using $T = 1.0$ is favorable for large-scale deployment. Regarding the sink block (shared prefix) size, we selected the system prompt by referring to the code provided by APE. For Star-Attention, we implemented its equivalent algorithm on a single node, with the anchor size

324 set equal to the context block size, following the setup in the Block-Attention paper (Ma et al., 2025).
 325 All methods use a context block size of 4096 tokens. Smaller context block sizes resulted in reduced
 326 accuracy for all methods, while larger blocks significantly degraded inference performance. To ensure
 327 fair comparison with baseline methods, PEVLM adopts identical 16-frame sink and context block
 328 sizes (approximately 4k tokens for Qwen2.5-VL and LongVILA, and 3k tokens for LLaVA-Video,
 329 Qwen3-VL and InternVL3_5).

330 4.1.2 RESULTS

331 As shown in Table 1 and the extended results in Appendix F, PEVLM consistently achieves the
 332 highest accuracy among all efficient-attention baselines across a wide range of models, datasets and
 333 video lengths. On the latest InternVL3_5, Qwen3-VL, and Qwen2.5-VL families, PEVLM remains
 334 close to Full Attention, while Block-Attention, APE, and Star-Attention exhibit substantial drops
 335 across nearly all evaluation tracks.

336 The same trend holds across model scales from 2B to 32B and across both dense and MoE variants:
 337 PEVLM preserves accuracy reliably, whereas the baselines degrade significantly as model size
 338 increases or when the evaluation involves longer videos. Furthermore, the radar graph analyzes in
 339 Appendix G show that PEVLM maintains strong performance on both temporally sensitive tasks
 340 and fine-grained visual details tasks, while alternative methods exhibit inconsistent behavior across
 341 categories.

342 For LongVILA and LLaVA-Video, although the accuracy gaps among parallel encoding schemes
 343 are generally smaller than those in the Qwen-VL and InternVL families, PEVLM still consistently
 344 performs best. Taken together, the results in both the main table and the appendix demonstrate that
 345 PEVLM is the most stable and effective parallel encoding approach across architectures, evaluation
 346 settings, and model scales.

347 4.2 PERFORMANCE EVALUATION

348 **Setup** The primary objective of this experiment is to assess the improvements in computational
 349 efficiency introduced by PEVLM. We conducted computational efficiency evaluations on the Qwen2.5-
 350 VL model. We built PEVLM based on SGLang, which is a fast serving framework for large language
 351 models and vision-language models, widely used in cloud production deployment (The corresponding
 352 code will be open-sourced on GitHub once internal compliance review is fully completed). All
 353 experiments were carried out on an NVIDIA H20-96G GPGPU. Given that PEVLM primarily
 354 optimizes the attention mechanism within the LLM, we measured the execution time of both the
 355 entire LLM module and its individual attention layers separately.

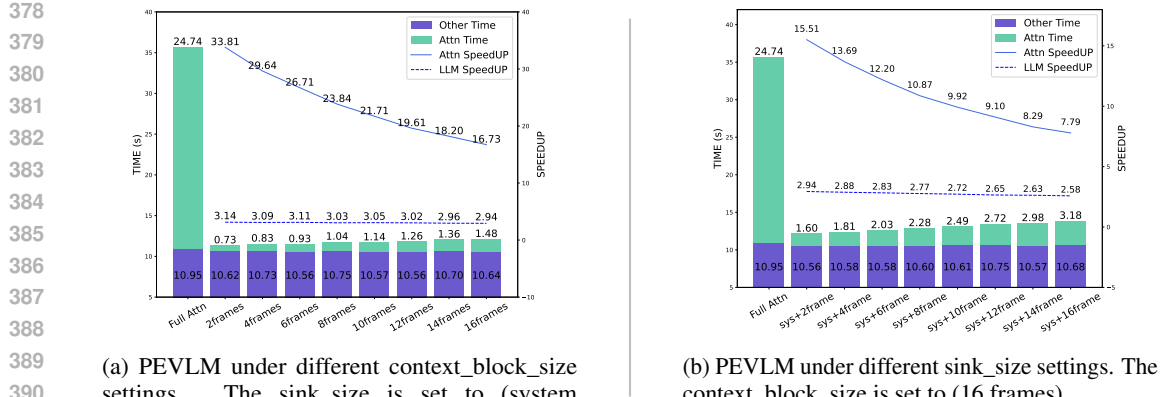
356 **Results** As shown in Figure 4, PEVLM reduces the end-to-end inference latency of the LLM by
 357 44% to 50%, depending on the block and sink sizes chosen. The acceleration is primarily driven by
 358 the attention module, which achieves speedups ranging from 7.79 \times to 33.81 \times , while the execution
 359 time of non-attention components remains largely unchanged.

360 As the sink block size or context block size increases, the speedup of the attention module gradually
 361 diminishes. This behavior is consistent with Equation 9, which indicates that the computational cost
 362 of attention grows quadratically with respect to the sizes of the sink and context blocks. Notably,
 363 because non-attention components account for a substantial portion of the total runtime, the overall
 364 end-to-end speedup degrades only moderately under larger block configurations.

365 However, when both context block size and sink block size increase to 16 frames, the fraction of
 366 time spent on attention rises sharply from 6.4% to 22.9%, suggesting that further enlarging the block
 367 size will lead to a more pronounced decline in overall system performance. We further analyze the
 368 trade-off between efficiency degradation and potential accuracy gains introduced by larger sink and
 369 context blocks in Section 5.

370 4.3 ACCURACY WITH LIMITED LATENCY

371 Deploying VLMs on edge devices presents significant challenges due to constrained computational
 372 resources and stringent latency requirements. Lacking native edge-testing infrastructure, we designed



(a) PEVLM under different context_block_size settings. The sink_size is set to (system prompt+one frame).

(b) PEVLM under different sink_size settings. The context_block_size is set to (16 frames).

Figure 4: Performance of PEVLM under different block size configurations: "Attn Time" refers to attention computation time, and "Other Time" covers all other LLM costs. "Attn SpeedUP" and "LLM SpeedUP" indicate the acceleration over Attention layer and overall LLM performance.

a latency-aware simulation to evaluate the practical benefits of PEVLM by emulating real-world deployment conditions on resource-limited devices.

Setup We adopt LongVideoBench as the evaluation benchmark and introduce a latency threshold during inference: Any sample that exceeds this latency limit is treated as a failure. All experiments are conducted on the NVIDIA H20-96G GPGPU. We use Qwen2.5-VL-7B-Instruct with Full-Attention as the primary baseline, and compare the performance of Full-Attention and PEVLM under identical latency constraints. To further reflect deployment in low-resource environments, where smaller models are commonly used to meet latency budgets, we also include comparisons with Qwen2.5-VL-3B-Instruct, a smaller variant Qwen2.5-VL-7B-Instruct.

Table 2: Accuracy \uparrow with Limited Latency

	Full Attn		PEVLM	
	sink	context	sys+2f	sys+16f
No Limit	60.43%	55.05%	61.18%	62.23%
40s	59.69%	55.05%	61.18%	62.23%
30s	27.08%	55.05%	61.18%	62.23%
20s	23.26%	24.38%	61.03%	60.28%

Results As shown in Table 2, the accuracy of Full-Attention (7B) drops sharply when the latency constraint is reduced from 40s to 30s, and the smaller Full-Attention (3B) model also shows a significant decline when the limit is further tightened to 20s. In contrast, PEVLM maintains consistently high accuracy even under the strictest 20s constraint. Notably, while the larger sink size (sys+16f) achieves the best accuracy under relaxed constraints (≥ 30 s), the smaller configuration (sys+2f) performs better under the 20s limit due to its lower latency overhead.

In general, PEVLM significantly improves accuracy in latency-constrained scenarios. Moreover, to maximize performance across diverse hardware and deployment conditions, the optimal configuration (e.g., sink/block size) should be adaptively tuned.

5 HOW DOES EACH COMPONENT IN PEVLM CONTRIBUTE TO THE PERFORMANCE?

Table 3 reports the ablation study across all five model families. The results show a clear and consistent trend. Adding SP yields the largest single-step improvement and forms the foundation

432 Table 3: Ablation study of PEVLM components
433

434 LongVideoBench								
435 SP	436 DF	437 FS	438 LLaVA-Video	439 LongVILA	440 Qwen2.5-VL	441 Qwen3-VL	442 InternVL3_5	443 AVG
			57.29	51.61	30.44	54.23	55.25	48.65
✓			57.82	52.58	59.84	60.21	57.27	56.88
✓	✓		57.97	52.95	60.06	61.09	59.05	57.51
✓	✓	✓	58.94	53.70	62.15	64.25	61.52	59.08
444 VideoMME								
445 SP	446 DF	447 FS	448 LLaVA-Video	449 LongVILA	450 Qwen2.5-VL	451 Qwen3-VL	452 InternVL3_5	453 AVG
			17.56	57.26	61.11	54.95	58.63	49.90
✓			61.78	58.00	61.74	62.93	60.31	60.95
✓	✓		62.07	57.30	62.52	64.99	64.23	62.22
✓	✓	✓	64.00	59.37	63.30	67.48	65.74	63.98

450 of PEVLM’s effectiveness. Introducing DF offers additional but smaller gains, improving stability
451 and accuracy across models. Incorporating FS provides the final boost, and combining all three
452 components results in the highest accuracy on every benchmark and every model family. Overall,
453 the three components are complementary, and the full PEVLM design provides the most robust and
454 reliable performance in long-video settings.

456 5.1 SEQUENTIAL POSITION EMBEDDING

457 We further analyze the component with the greatest impact on accuracy: the preservation of sequential
458 position embeddings. As discussed before, adopting sequential position embeddings instead of
459 reusing position embeddings across context blocks produces attention distributions that more closely
460 resemble those of Full-Attention, thereby aligning better with the model’s expected behavior. As
461 shown in Table 4, the use of sequential position embeddings significantly improves accuracy in both
462 Qwen2.5-VL and LongVILA. In contrast, for the LLaVA-Video model, the benefit is marginal, likely
463 because its attention score distribution (as shown in Figure 10 in the Appendix H) remains relatively
464 stable even when using parallel encoding.

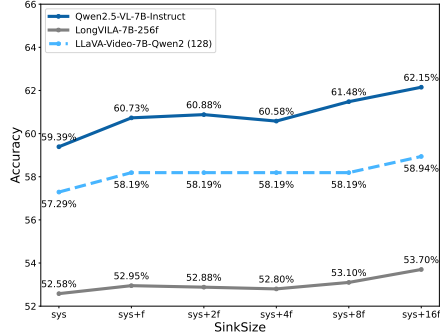
466 Table 4: Accuracy \uparrow on LongVideoBench dataset with Different Position Embedding Strategy

469 model	470 method	471 reuse pos	472 sequential
Qwen2.5-VL- 7B-Instruct	APE (T=1.0)	30.44%	59.39%
	Star Attn	29.54%	61.41%
	PEVLM	14.73%	62.23%
LongVILA- 7B-256f	APE (T=1.0)	51.46%	53.40%
	Star Attn	51.76%	53.63%
	PEVLM	49.96%	53.70%
LLaVA-Video- 7B-Qwen2	APE (T=1.0)	58.19%	58.12%
	Star Attn	58.71%	58.49%
	PEVLM	58.34%	59.01%

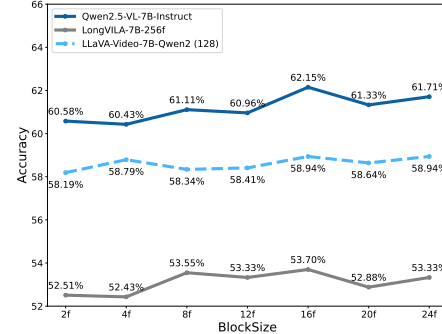
482 5.2 SINK & CONTEXT BLOCK SIZE

483 As analyzed in the *PEVLM* section, the inference latency of PEVLM grows quadratically with the
484 sizes of both the sink and context blocks, which aligns with the empirical results shown in Figure 4.
485 We further investigate how these block sizes affect the accuracy of parallel encoding.

486
487 First, as noted in the *Observations* section, including the initial frames of the video in the sink
488 is crucial. This is validated in Figure 5, where incorporating early frames into the sink leads to
489 noticeable accuracy improvements across all models evaluated.
490



502 The impact of sink sizes on accuracy. The x-
503 axis shows different sink size configurations from
504 system prompt (sys) to system prompt plus 16 frames
505 (sys+16f).



506 The impact of context block sizes on accuracy. The x-
507 axis shows different context block size configurations from
508 2 frames (2f) to 24 frames (24f).

509 Figure 5: The impact of sink&block sizes on accuracy.

510 Figure 5 also shows that model accuracy generally increases with sink size. However, due to
511 the quadratic latency growth, large sink sizes are not ideal for deployment. Therefore, a simple
512 pre-deployment test may be necessary to determine the optimal configuration. Since there is no
513 one-size-fits-all solution for determining the best configuration, users should make their choice based
514 on actual requirements. For example, when latency constraints are considered, as shown in Table 2,
515 under a 20-second latency budget, using only [SYS] + 2 frames as the Sink Block yields higher
516 accuracy than [SYS] + 16 frames.

517 We also examine the effect of context block size on model accuracy. As shown in Figure 5, increasing
518 the size of context blocks leads to consistent accuracy gains, similar to the trend observed with the
519 sink block size. However, Figure 4 reveals that latency also increases quadratically with block size,
520 further emphasizing the trade-off between accuracy and computational efficiency.

6 CONCLUSION

521 We introduce PEVLM, a fine-tuning-free parallel encoding strategy that significantly accelerates
522 Vision-Language Models for long-video understanding. By preserving sequential position
523 embeddings and leveraging a shared Sink Block, PEVLM aligns attention behavior with Full-
524 Attention while reducing complexity from $O((T \times N)^2)$ to $O(T \times N)$. It achieves up to $7.47 \times$
525 attention speed-up, 44% to 50% end-to-end latency reduction, and strong accuracy gains under tight
526 latency constraints. PEVLM offers a practical and scalable solution for multimodal real-world and
527 long-context tasks.

REPRODUCIBILITY STATEMENT

528 To ensure the reproducibility of our work, we have detailed the experimental methodology for
529 PEVLM in Section 3, providing a clear description of its partitioning strategy, formulations, and
530 block size considerations. Additionally, Section 4.1, Sections 4.2 and Section 4.3 further specify the
531 comparative evaluation settings, detailing computational efficiency tests on the NVIDIA H20-96G
532 GPGPU using the SGLang framework and latency-constrained simulations, respectively. These
533 comprehensive details enable other researchers to replicate and validate our findings. We will also
534 release the project code based on SGLang in the near future.

540 REVISION NOTE
541542 In response to reviewer feedback, we have significantly expanded our experimental evaluation and
543 clarified key aspects of our method. Specifically:
544

- 545 We extended experiments to include the latest InternVL3.5 and Qwen3-VL model families,
546 covering architectures from 2B to 32B parameters (both dense and MoE), and evaluated them
547 across five long-video benchmarks (MVBench, EgoSchema, VideoMME, LongVideoBench,
548 MME-VideoOCR), confirming PEVLM’s robustness across scales and fine-grained tasks
549 such as video OCR;
- 550 We conducted comprehensive ablation studies across multiple model families, demonstrating
551 that each of PEVLM’s three components—Sequential Position Embedding, Divide by Frame,
552 and Frame Sink—consistently contributes to accuracy;
- 553 We corrected a citation error (Line 202), fixed typographical issues throughout the
554 manuscript, and regenerated Figures 3 and 4 in higher resolution to improve clarity.

555 These revisions strengthen both the empirical foundation and presentation of our work, further
556 validating PEVLM as an effective, training-free solution for accelerating long-video inference in
557 vision-language models.
558559 REFERENCES
560

561 Shantanu Acharya, Fei Jia, and Boris Ginsburg. Star attention: Efficient llm inference over long
562 sequences, 2025. URL <https://arxiv.org/abs/2411.17116>.

563 J. B. Alayrac et al. Flamingo: A visual language model for few-shot learning. *arXiv preprint*, 2022.

564 Shuai Bai, Keqin Chen, Xuejing Liu, Jialin Wang, Wenbin Ge, Sibo Song, Kai Dang, Peng Wang,
565 Shijie Wang, Jun Tang, Humen Zhong, Yuanzhi Zhu, Mingkun Yang, Zhaohai Li, Jianqiang Wan,
566 Pengfei Wang, Wei Ding, Zheren Fu, Yiheng Xu, Jiabo Ye, Xi Zhang, Tianbao Xie, Zesen Cheng,
567 Hang Zhang, Zhibo Yang, Haiyang Xu, and Junyang Lin. Qwen2.5-vl technical report, 2025. URL
568 <https://arxiv.org/abs/2502.13923>.

569 I. Beltagy, M. E. Peters, and A. Cohan. Longformer: The long-document transformer. *arXiv preprint*,
570 2020.

571 Kevin Black, Noah Brown, Danny Driess, Adnan Esmail, Michael Equi, Chelsea Finn, Niccolò Fusai,
572 Lachy Groom, Karol Hausman, Brian Ichter, Szymon Jakubczak, Tim Jones, Liyiming Ke, Sergey
573 Levine, Adrian Li-Bell, Mohith Mothukuri, Suraj Nair, Karl Pertsch, Lucy Xiaoyang Shi, James
574 Tanner, Quan Vuong, Anna Walling, Haohuan Wang, and Ury Zhilinsky. π_0 : A vision-language-
575 action flow model for general robot control, 2024. URL <https://arxiv.org/abs/2410.24164>.

576 Yukang Chen, Fuzhao Xue, Dacheng Li, Qinghao Hu, Ligeng Zhu, Xiuyu Li, Yunhao Fang, Haotian
577 Tang, Shang Yang, Zhijian Liu, Ethan He, Hongxu Yin, Pavlo Molchanov, Jan Kautz, Linxi Fan,
578 Yuke Zhu, Yao Lu, and Song Han. Longvila: Scaling long-context visual language models for long
579 videos, 2024. URL <https://arxiv.org/abs/2408.10188>.

580 Jiayu Ding, Shuming Ma, Li Dong, Xingxing Zhang, Shaohan Huang, Wenhui Wang, Nanning
581 Zheng, and Furu Wei. Longnet: Scaling transformers to 1,000,000,000 tokens, 2023. URL
582 <https://arxiv.org/abs/2307.02486>.

583 Chaoyou Fu, Yuhan Dai, Yondong Luo, Lei Li, Shuhuai Ren, Renrui Zhang, Zihan Wang, Chenyu
584 Zhou, Yunhang Shen, Mengdan Zhang, et al. Video-mme: The first-ever comprehensive evaluation
585 benchmark of multi-modal llms in video analysis. *arXiv preprint arXiv:2405.21075*, 2024.

586 Lei Gao, Chunyuan Lin, et al. Perception and planning with long context vlms. *arXiv preprint*
587 *arXiv:2403.07698*, 2024.

588 Junqi Ge, Ziyi Chen, Jintao Lin, Jinguo Zhu, Xihui Liu, Jifeng Dai, and Xizhou Zhu. V2pe:
589 Improving multimodal long-context capability of vision-language models with variable visual
590 position encoding, 2024. URL <https://arxiv.org/abs/2412.09616>.

594 K. Guu et al. Retrieval-augmented language model pretraining. In *ICML*, 2020.
 595

596 Yujie Hu, Zonglin Wu, et al. Drivevlm: Adaptive vision-language modeling for autonomous driving.
 597 *arXiv preprint arXiv:2311.09876*, 2023.

598 Qidong Huang, Xiaoyi Dong, Pan Zhang, Bin Wang, Conghui He, Jiaqi Wang, Dahua Lin, Weiming
 599 Zhang, and Nenghai Yu. Opera: Alleviating hallucination in multi-modal large language models
 600 via over-trust penalty and retrospection-allocation. In *Proceedings of the IEEE/CVF Conference*
 601 *on Computer Vision and Pattern Recognition*, pp. 13418–13427, 2024.

602

603 Seil Kang, Jinyeong Kim, Junhyeok Kim, and Seong Jae Hwang. See what you are told: Visual
 604 attention sink in large multimodal models, 2025. URL <https://arxiv.org/abs/2503.03321>.

605

606 MIT-HAN Lab and Meta AI. Streamingllm: Enabling infinite-length generation with attention sinks.
 607 *arXiv preprint arXiv:2309.17453*, 2023. URL <https://arxiv.org/abs/2309.17453>.

608

609 Xunhao Lai, Jianqiao Lu, Yao Luo, Yiyuan Ma, and Xun Zhou. Flexprefill: A context-aware sparse
 610 attention mechanism for efficient long-sequence inference, 2025. URL <https://arxiv.org/abs/2502.20766>.

611

612 Kunchang Li, Yali Wang, Yinan He, Yizhuo Li, Yi Wang, Yi Liu, Zun Wang, Jilan Xu, Guo Chen, Ping
 613 Luo, Limin Wang, and Yu Qiao. Mvbench: A comprehensive multi-modal video understanding
 614 benchmark, 2024a. URL <https://arxiv.org/abs/2311.17005>.

615

616 Xiuju Li, Xi Yin, Chunyuan Li, Xiaowei Hu, Pengchuan Zhang, Lei Zhang, Lijuan Wang, Houdong
 617 Hu, Li Dong, Furu Wei, et al. Oscar: Object-semantics aligned pre-training for vision-language
 618 tasks. In *ECCV*, 2020.

619

620 Zhenyu Li, Yike Zhang, Tengyu Pan, Yutao Sun, Zhichao Duan, Junjie Fang, Rong Han, Zixuan Wang,
 621 and Jianyong Wang. Focusllm: Precise understanding of long context by dynamic condensing,
 622 2024b. URL <https://arxiv.org/abs/2408.11745>.

623

624 Nelson F. Liu, Kevin Lin, John Hewitt, Ashwin Paranjape, Michele Bevilacqua, Fabio Petroni,
 625 and Percy Liang. Lost in the middle: How language models use long contexts. *Transactions*
 626 *of the Association for Computational Linguistics*, 12:157–173, 2023. URL <https://api.semanticscholar.org/CorpusID:259360665>.

627

628 Xiangrui Liu, Yan Shu, Zheng Liu, Ao Li, Yang Tian, and Bo Zhao. Video-xl-pro: Reconstructive
 629 token compression for extremely long video understanding. *arXiv preprint arXiv:2503.18478*,
 630 2025.

631

632 Xiaohui Liu, Wei Zhang, et al. Bmed-vl: A vision-language model for multimodal biomedical
 633 reasoning. *arXiv preprint arXiv:2401.04512*, 2024.

634

635 Enzhe Lu, Zhejun Jiang, Jingyuan Liu, Yulun Du, Tao Jiang, Chao Hong, Shaowei Liu, Weiran He,
 636 Enming Yuan, Yuzhi Wang, Zhiqi Huang, Huan Yuan, Suting Xu, Xinran Xu, Guokun Lai, Yanru
 637 Chen, Huabin Zheng, Junjie Yan, Jianlin Su, Yuxin Wu, Neo Y. Zhang, Zhilin Yang, Xinyu Zhou,
 638 Mingxing Zhang, and Jiezhong Qiu. Moba: Mixture of block attention for long-context llms, 2025.
 639 URL <https://arxiv.org/abs/2502.13189>.

640

641 Songshuo Lu, Hua Wang, Yutian Rong, Zhi Chen, and Yaohua Tang. Turborag: Accelerating
 642 retrieval-augmented generation with precomputed kv caches for chunked text, 2024. URL <https://arxiv.org/abs/2410.07590>.

643

644 Hao Luo, Yicheng Feng, Wanpeng Zhang, Sipeng Zheng, Ye Wang, Haoqi Yuan, Jiazheng Liu, Chaoyi
 645 Xu, Qin Jin, and Zongqing Lu. Being-h0: Vision-language-action pretraining from large-scale
 646 human videos, 2025. URL <https://arxiv.org/abs/2507.15597>.

647

Dongyang Ma, Yan Wang, and Lan Tian. Block-attention for efficient prefilling, 2025. URL
<https://arxiv.org/abs/2409.15355>.

648 Kartikeya Mangalam, Raiymbek Akshulakov, and Jitendra Malik. Egoschema: A diagnostic
 649 benchmark for very long-form video language understanding. In A. Oh, T. Naumann,
 650 A. Globerson, K. Saenko, M. Hardt, and S. Levine (eds.), *Advances in Neural Information
 651 Processing Systems*, volume 36, pp. 46212–46244. Curran Associates, Inc., 2023. URL
 652 https://proceedings.neurips.cc/paper_files/paper/2023/file/90ce332aff156b910b002ce4e6880dec-Paper-Datasets_and_Benchmarks.pdf.
 653

654 Arka Pal, Deep Karkhanis, Manley Roberts, Samuel Dooley, Arvind Sundararajan, and Siddartha
 655 Naidu. Giraffe: Adventures in expanding context lengths in llms, 2023. URL <https://arxiv.org/abs/2308.10882>.
 656

657 Minghao Qin, Xiangrui Liu, Zhengyang Liang, Yan Shu, Huaying Yuan, Juenjie Zhou, Shitao Xiao,
 658 Bo Zhao, and Zheng Liu. Video-xl-2: Towards very long-video understanding through task-aware
 659 kv sparsification. *arXiv preprint arXiv:2506.19225*, 2025.

660 Nir Ratner, Yoav Levine, Yonatan Belinkov, Ori Ram, Inbal Magar, Omri Abend, Ehud Karpas,
 661 Amnon Shashua, Kevin Leyton-Brown, and Yoav Shoham. Parallel context windows for large
 662 language models, 2023. URL <https://arxiv.org/abs/2212.10947>.
 663

664 Yang Shi, Huanqian Wang, Wulin Xie, Huanyao Zhang, Lijie Zhao, Yi-Fan Zhang, Xinfeng Li,
 665 Chaoyou Fu, Zhuoer Wen, Wenting Liu, Zhuoran Zhang, Xinlong Chen, Bohan Zeng, Sihan Yang,
 666 Yuanxing Zhang, Pengfei Wan, Haotian Wang, and Wenjing Yang. Mme-videoocr: Evaluating
 667 ocr-based capabilities of multimodal llms in video scenarios, 2025. URL <https://arxiv.org/abs/2505.21333>.
 668

669 Yan Shu, Peitian Zhang, Zheng Liu, Minghao Qin, Junjie Zhou, Tiejun Huang, and Bo Zhao.
 670 Video-xl: Extra-long vision language model for hour-scale video understanding. *arXiv preprint
 671 arXiv:2409.14485*, 2024.

672

673 Mingjie Sun, Xinlei Chen, J. Zico Kolter, and Zhuang Liu. Massive activations in large language
 674 models, 2024. URL <https://arxiv.org/abs/2402.17762>.
 675

676 Gemini Robotics Team, Saminda Abeyruwan, Joshua Ainslie, Jean-Baptiste Alayrac,
 677 Montserrat Gonzalez Arenas, Travis Armstrong, Ashwin Balakrishna, Robert Baruch, Maria
 678 Bauza, Michiel Blokzijl, Steven Bohez, Konstantinos Bousmalis, Anthony Brohan, Thomas
 679 Buschmann, Arunkumar Byravan, Serkan Cabi, Ken Caluwaerts, Federico Casarini, Oscar Chang,
 680 Jose Enrique Chen, Xi Chen, Hao-Tien Lewis Chiang, Krzysztof Choromanski, David D'Ambrosio,
 681 Sudeep Dasari, Todor Davchev, Coline Devin, Norman Di Palo, Tianli Ding, Adil Dostmohamed,
 682 Danny Driess, Yilun Du, Debidatta Dwibedi, Michael Elabd, Claudio Fantacci, Cody Fong,
 683 Erik Frey, Chuyuan Fu, Marissa Giustina, Keerthana Gopalakrishnan, Laura Graesser, Leonard
 684 Hasenklever, Nicolas Heess, Brandon Hernaez, Alexander Herzog, R. Alex Hofer, Jan Humplik,
 685 Atil Iscen, Mithun George Jacob, Deepali Jain, Ryan Julian, Dmitry Kalashnikov, M. Emre
 686 Karagozler, Stefani Karp, Chase Kew, Jerad Kirkland, Sean Kirmani, Yuheng Kuang, Thomas
 687 Lampe, Antoine Laurens, Isabel Leal, Alex X. Lee, Tsang-Wei Edward Lee, Jacky Liang, Yixin
 688 Lin, Sharath Maddineni, Anirudha Majumdar, Assaf Hurwitz Michaely, Robert Moreno, Michael
 689 Neunert, Francesco Nori, Carolina Parada, Emilio Parisotto, Peter Pastor, Acorn Pooley, Kanishka
 690 Rao, Krista Reymann, Dorsa Sadigh, Stefano Saliceti, Pannag Sanketi, Pierre Sermanet, Dhruv
 691 Shah, Mohit Sharma, Kathryn Shea, Charles Shu, Vikas Sindhwani, Sumeet Singh, Radu Soricut,
 692 Jost Tobias Springenberg, Rachel Sterneck, Razvan Surdulescu, Jie Tan, Jonathan Tompson,
 693 Vincent Vanhoucke, Jake Varley, Grace Vesom, Giulia Vezzani, Oriol Vinyals, Ayzaan Wahid,
 694 Stefan Welker, Paul Wohlhart, Fei Xia, Ted Xiao, Annie Xie, Jinyu Xie, Peng Xu, Sichun Xu, Ying
 695 Xu, Zhuo Xu, Yuxiang Yang, Rui Yao, Sergey Yaroshenko, Wenhao Yu, Wentao Yuan, Jingwei
 696 Zhang, Tingnan Zhang, Allan Zhou, and Yuxiang Zhou. Gemini robotics: Bringing ai into the
 697 physical world, 2025. URL <https://arxiv.org/abs/2503.20020>.
 698

699 Qwen Team. Qwen3 technical report, 2025. URL <https://arxiv.org/abs/2505.09388>.
 700

701 Ashish Vaswani, Noam Shazeer, Niki Parmar, Jakob Uszkoreit, Llion Jones, Aidan N Gomez, Łukasz
 702 Kaiser, and Illia Polosukhin. Attention is all you need. *Advances in neural information processing
 703 systems*, 30, 2017.

702 Petar Veličković, Christos Perivolaropoulos, Federico Barbero, and Razvan Pascanu. Softmax is
 703 not enough (for sharp size generalisation), 2025. URL <https://arxiv.org/abs/2410.01104>.

704

705 Ming Wang, Tianyu Zhao, et al. Cascaded multimodal transformers for driving video analysis. *arXiv
 706 preprint arXiv:2401.05678*, 2024.

707

708 Weiyun Wang, Zhangwei Gao, Lixin Gu, Hengjun Pu, Long Cui, Xingguang Wei, Zhaoyang Liu,
 709 Linglin Jing, Shenglong Ye, Jie Shao, et al. Internvl3.5: Advancing open-source multimodal
 710 models in versatility, reasoning, and efficiency. *arXiv preprint arXiv:2508.18265*, 2025a.

711

712 Xidong Wang, Dingjie Song, Shunian Chen, Junyin Chen, Zhenyang Cai, Chen Zhang, Lichao Sun,
 713 and Benyou Wang. Longllava: Scaling multi-modal llms to 1000 images efficiently via a hybrid
 714 architecture, 2025b. URL <https://arxiv.org/abs/2409.02889>.

715

716 Ruyi Xu, Guangxuan Xiao, Haofeng Huang, Junxian Guo, and Song Han. Xattention: Block sparse
 717 attention with antidiagonal scoring, 2025. URL <https://arxiv.org/abs/2503.16428>.

718

719 Xinyu Yang, Tianqi Chen, and Beidi Chen. Ape: Faster and longer context-augmented generation via
 adaptive parallel encoding, 2025. URL <https://arxiv.org/abs/2502.05431>.

720

721 Howard Yen, Tianyu Gao, and Danqi Chen. Long-context language modeling with parallel context
 722 encoding, 2024. URL <https://arxiv.org/abs/2402.16617>.

723

724 Jingyang Yuan, Huazuo Gao, Damai Dai, Junyu Luo, Liang Zhao, Zhengyan Zhang, Zhenda Xie,
 725 Y. X. Wei, Lean Wang, Zhiping Xiao, Yuqing Wang, Chong Ruan, Ming Zhang, Wenfeng Liang,
 726 and Wangding Zeng. Native sparse attention: Hardware-aligned and natively trainable sparse
 727 attention, 2025. URL <https://arxiv.org/abs/2502.11089>.

728

729 Jintao Zhang, Chendong Xiang, Haofeng Huang, Jia Wei, Haocheng Xi, Jun Zhu, and Jianfei Chen.
 730 SpARGEattention: Accurate and training-free sparse attention accelerating any model inference,
 731 2025a. URL <https://arxiv.org/abs/2502.18137>.

732

733 Kaichen Zhang, Bo Li, Peiyuan Zhang, Fanyi Pu, Joshua Adrian Cahyono, Kairui Hu, Shuai Liu,
 734 Yuanhan Zhang, Jingkang Yang, Chunyuan Li, and Ziwei Liu. Lmms-eval: Reality check on
 735 the evaluation of large multimodal models. In *Findings of the Association for Computational
 736 Linguistics: NAACL 2025*, pp. 881–916. Association for Computational Linguistics, 2025b. doi:
 737 10.18653/v1/2025.findings-naacl.51. URL <http://dx.doi.org/10.18653/v1/2025.findings-naacl.51>.

738

739 Peiyuan Zhang, Kaichen Zhang, Bo Li, Guangtao Zeng, Jingkang Yang, Yuanhan Zhang, Ziyue
 740 Wang, Haoran Tan, Chunyuan Li, and Ziwei Liu. Long context transfer from language to vision.
 741 *arXiv preprint arXiv:2406.16852*, 2024a. URL <https://arxiv.org/abs/2406.16852>.

742

743 T. Zhang and K. Wang. Longvideobench: Evaluating long video understanding for vlms. In
 744 *Conference on Neural Information Processing Systems (NeurIPS)*, 2024.

745

746 Xiaofeng Zhang, Yihao Quan, Chaochen Gu, Chen Shen, Xiaosong Yuan, Shaotian Yan, Hao Cheng,
 747 Kaijie Wu, and Jieping Ye. Seeing clearly by layer two: Enhancing attention heads to alleviate
 748 hallucination in lvlms, 2024b. URL <https://arxiv.org/abs/2411.09968>.

749

750 Yuanhan Zhang, Jinming Wu, Wei Li, Bo Li, Zejun Ma, Ziwei Liu, and Chunyuan Li. Video
 751 instruction tuning with synthetic data, 2024c. URL <https://arxiv.org/abs/2410.02713>.

752

753

754

755

APPENDIX

A RELATED WORK

Parallel Encoding Mechanisms. Several state-of-the-art architectural improvements have been proposed to improve parallel encoding. Adaptive Parallel Encoding (APE) aligns the attention score distribution of parallel encoding with sequential attention, but its hyperparameters are highly sensitive to input samples, complicating deployment (Yang et al., 2025). Star Attention reduces prefilling latency by parallel design but is tailored for distributed systems, limiting its use in single-node and edge devices (Acharya et al., 2025). Block-Attention & TurboRAG improve accuracy through position reencoding, but require fine-tuning due to the lack of handling for attention sink phenomena (Guu et al., 2020; Lu et al., 2024). Video-XL-2 (Qin et al., 2025) summarizes historical frame information to reduce kv-cache size during video prefilling and employs chunk-based prefilling to further accelerate processing. While effective, this inevitably compresses historical content and therefore introduces potential information loss. Other methods like Native Sparse Attention and MoBA achieve similar speed-ups but require architectural changes and full retraining (Yuan et al., 2025; Lu et al., 2025).

Efficient Attention Mechanisms. A growing body of work focuses on improving the efficiency of attention mechanisms for long sequences. StreamingLLM (Lab & AI, 2023) mitigates the "attention sink" phenomenon via fixed-pattern attention that selectively retains sink and sliding-window tokens. LongNet (Ding et al., 2023) introduces dilated attention, achieving linear complexity in sequence length. FlexPrefill (Lai et al., 2025) dynamically adapts attention patterns and computational budgets during inference. XAttention (Xu et al., 2025) predicts block importance via antidiagonal scoring, enabling sparsification with minimal accuracy loss. SpargeAttn (Zhang et al., 2025a) performs double-stage block-level filtering to achieve extreme prefill efficiency. These methods demonstrate the potential of sparsity- or pattern-driven attention to reduce computation, but they do not specifically target long-video prefilling scenarios, where frame-level ordering and large-scale multimodal inputs present additional challenges.

Long-Context VLMs. Recent multimodal research has pushed the context length of vision-language models to hundreds of thousands of tokens. LongVA (Zhang et al., 2024a), Qwen-VL/Qwen3-VL (Team, 2025), and LongVILA (Chen et al., 2024) extend multimodal Transformers to 128K tokens with new training and architecture strategies. LongLLaVA (Wang et al., 2025b) combines Mamba and Transformer blocks for memory-efficient long-context reasoning. GIRAFFE (Pal et al., 2023) introduces optimized data pipelines and positional schemes for extreme context lengths. V2PE (Ge et al., 2024) proposes variable-position visual encodings to enhance long-range multimodal representation. Video-XL (Shu et al., 2024) and Video-XL-2 (Liu et al., 2025) develop lightweight long-video modeling frameworks based on chunked prefilling, KV-cache sparsification, and dynamic token synthesis. These advances demonstrate substantial progress in long-context multimodal modeling; however, most focus on architectural scalability or training strategies rather than efficient, accuracy-preserving parallel encoding during the prefill stage. Our work addresses this gap by designing a parallel encoding scheme tailored for long-video processing.

B FUTURE WORK

Although PEVLM achieves notable gains in efficiency and performance for long video tasks, several directions remain open for exploration. First, we aim to extend PEVLM to richer multimodal inputs (e.g., LiDAR, maps, IMU) commonly used in robotics and autonomous systems, which pose unique challenges for alignment and fusion. Second, PEVLM is inherently better suited for streaming and online updates, as it computes only intra-frame attention and decouples inter-frame dependencies. This design supports causal real-time processing without requiring continuous updates, substantially reducing latency in VLM/VLA systems; building on this property, adapting PEVLM to online streaming settings that process only newly arrived data within a sliding window could further enable real-time reasoning with significant speed-ups. Lastly, we plan to investigate the theoretical reasons behind the performance gains of parallel encoding over Full-Attention, potentially uncovering deeper insights for modeling long contexts.

810 C THE USE OF LARGE LANGUAGE MODELS (LLMs) 811

812 LLMs were used in this work only for spelling correction, grammar improvement, and language
813 polishing. No content was generated by LLMs for research ideation, experimental design, data
814 analysis, or substantive scientific contribution. All research decisions and substantive writing remain
815 the sole responsibility of the authors.

817 D BENCHMARK DETAILS 818

819 We evaluate our method on several video understanding benchmarks that test different aspects of
820 video comprehension:

823 D.1 EGOSCHEMA [NEURIPS 2023]

824 EgoSchema (Mangalam et al., 2023) is a large-scale benchmark designed to evaluate multimodal
825 Large Language Models (MLLMs) on egocentric video understanding. It consists of 100 hours of
826 first-person video data spanning 1,270 daily activity episodes across diverse real-world environments.
827 The benchmark introduces over 10,000 manually curated question-answer pairs, covering tasks such
828 as object grounding, human-object interaction, activity reasoning, and intent prediction.

830 D.2 MVBENCH [CVPR 2024]

832 MVBench (Li et al., 2024a) is a comprehensive benchmark designed to evaluate multimodal
833 Large Language Models (MLLMs) on multi-granular video understanding. It consists of 5
834 task categories—including moment-level, frame-level, clip-level, video-level, and holistic video
835 understanding—covering a wide range of temporal scopes and reasoning demands. The benchmark
836 includes 2,562 manually annotated questions grounded in 4,119 diverse video clips, selected from
837 real-world scenarios.

838 Each question is carefully designed to probe different levels of spatiotemporal understanding,
839 from fine-grained object recognition and short-term motion tracking to long-term event inference.
840 MVBench offers a unified and challenging evaluation protocol to assess the generalization and
841 reasoning ability of MLLMs across granularities.

842 Unlike conventional third-person video datasets, EgoSchema emphasizes embodied perception
843 and temporal reasoning from an egocentric perspective, posing unique challenges for spatial
844 understanding, long-term memory, and causal inference in MLLMs.

846 D.3 VIDEO-MME [CVPR 2025]

848 Video-MME (Fu et al., 2024) is a comprehensive evaluation benchmark for assessing the video
849 understanding capabilities of multimodal Large Language Models (MLLMs). It spans 6 primary
850 visual domains and 30 subfields, covering a diverse range of video types and temporal scenarios. The
851 benchmark includes 900 videos with durations ranging from 11 seconds to 1 hour, totaling 254 hours
852 of content.

853 To evaluate fine-grained visual and temporal reasoning, 2,700 manually annotated question-answer
854 pairs are provided. Video-MME challenges models to comprehend both short and long video clips
855 across different temporal granularities, making it a rigorous benchmark for evaluating the core video
856 processing capabilities of MLLMs.

858 D.4 LONGVIDEOBENCH [NEURIPS 2024]

860 LongVideoBench (Zhang & Wang, 2024) is a benchmark specifically designed to evaluate the
861 long-context video understanding capabilities of multimodal Large Language Models (MLLMs). It
862 features 1,760 videos spanning 12 diverse real-world scenarios, with video durations ranging from 5
863 minutes to 2 hours, totaling over 1,000 hours of content. The benchmark includes 2,400 manually
864 annotated multi-choice questions targeting key aspects of long video comprehension.

864 LongVideoBench focuses on challenging long-range temporal reasoning, event tracking, and global
 865 understanding across extended video content. It aims to assess whether models can maintain
 866 coherence, memory, and attention over prolonged contexts, making it a rigorous testbed for long-form
 867 video modeling.

869 D.5 MME-VIDEOOCR [NEURIPS 2025]

871 MME-VideoOCR (Shi et al., 2025) evaluates video-based OCR capabilities in MLLMs. It contains
 872 1,464 videos across 44 scenarios, with 2,000 manually annotated QA pairs covering 10 task categories
 873 and 25 sub-tasks. The benchmark stresses challenges unique to video OCR, including motion blur,
 874 frame variation, and spatio-temporal text integration.

875 It assesses models on fine-grained text recognition, cross-frame aggregation, structured text parsing,
 876 and reasoning over dynamic visual content. Results on 18 state-of-the-art MLLMs show that video
 877 OCR remains difficult—top models reach only 73.7% accuracy. Performance notably drops on tasks
 878 requiring holistic temporal understanding or robustness against language priors, underscoring the
 879 need for high-resolution inputs and sufficient temporal coverage.

881 E ABLATION STUDY OF PEVLM COMPONENTS

884 Table 5: Ablation study of PEVLM components (Qwen3-VL models)

886 SP	887 DF	888 FS	LongVideoBench (%)					VideoMME (%)				
			889 AVG	890 2B	891 4B	892 8B	893 32B	894 AVG	895 2B	896 4B	897 8B	898 32B
			54.23	46.07	51.91	59.76	59.16	54.95	43.19	50.04	59.41	67.19
✓			60.21	55.72	60.58	61.71	62.83	62.93	56.26	61.37	64.04	70.07
✓	✓		61.09	56.54	61.33	62.60	63.87	64.99	58.59	63.41	66.96	71.00
✓	✓	✓	64.25	58.49	64.77	66.49	67.24	67.48	60.22	67.11	69.48	73.11

894 Table 6: Ablation study of PEVLM components (InternVL3_5 models)

896 SP	897 DF	898 FS	LongVideoBench (%)					VideoMME (%)				
			899 AVG	900 4B	901 8B	902 14B	903 30B-A3B	904 AVG	905 4B	906 8B	907 14B	908 30B-A3B
			55.25	53.10	54.90	55.72	57.29	58.63	56.41	57.81	57.81	62.48
✓			57.27	55.42	56.92	57.89	58.86	60.31	58.07	58.48	61.44	63.26
✓	✓		59.05	58.49	58.26	59.01	60.43	64.23	62.33	62.70	65.81	66.04
✓	✓	✓	61.52	59.69	62.00	61.93	62.45	65.74	63.33	64.74	67.44	67.44

903 We conduct ablation experiments to quantify the contribution of the three components of PEVLM:
 904 Sequential Position alignment (SP), Divide-by-Frame (DF), and the Frame Sink mechanism (FS).
 905 Results for Qwen3-VL and InternVL3_5 are shown in Tables 5 and 6.

906 Across both model families, the baseline without any components yields the lowest accuracy.
 907 Introducing SP brings the largest single-step improvement. Adding DF provides further consistent
 908 gains across all model scales. Incorporating FS delivers the final boost, and the full combination
 909 (SP+DF+FS) achieves the highest accuracy in every benchmark.

910
 911 Overall, the ablation results show that each component contributes positively and that all three
 912 together form a complementary and effective design for stable parallel video encoding.

914 F BENCHMARK RESULTS OF QWEN3-VL AND INTERNVL3_5

915 Tables 7 and 8 provide a comprehensive comparison of efficient attention mechanisms across eight
 916 model checkpoints. Two consistent empirical findings emerge.

918 Table 7: Performance (\uparrow) of Qwen3-VL models with different methods on video understanding tasks
 919 evaluated at tokens from 26k to 100k.

921 Method	922 MVBench 17s avg.	923 EgoSchema 3m avg.	924 VideoMME < 2m	925 2m-1h	926 LongVideoBench < 1m	927 1m-1h	928 VideoOCR 34s avg.	929 Avg.
930 Qwen3-VL-2B-Instruct								
931 Full Attn	63.28%	60.80%	75.33%	55.94%	71.75%	53.07%	58.26%	62.63%
932 Block Attn (ICLR25)	61.72%	58.20%	57.78%	45.44%	64.82%	44.77%	54.21%	55.28%
933 APE (ICLR25)	48.06%	58.80%	30.00%	49.78%	36.29%	49.69%	45.74%	45.48%
934 Star Attn (ICML25)	52.42%	2.00%	8.78%	52.83%	46.26%	46.93%	46.10%	36.47%
935 PEVLM	63.25%	61.80%	74.11%	53.28%	73.13%	53.07%	58.05%	62.38%
936 Qwen3-VL-4B-Instruct								
937 Full Attn	67.14%	70.60%	79.00%	65.67%	78.67%	62.70%	62.87%	69.52%
938 Block Attn (ICLR25)	65.39%	66.20%	63.67%	51.22%	74.52%	52.25%	60.10%	61.91%
939 APE (ICLR25)	53.86%	66.80%	43.11%	53.50%	45.15%	54.41%	45.95%	51.83%
940 Star Attn (ICML25)	57.22%	11.00%	20.22%	57.50%	52.08%	57.48%	51.49%	43.86%
941 PEVLM	67.11%	71.00%	78.78%	61.28%	78.67%	59.63%	62.87%	68.48%
942 Qwen3-VL-8B-Instruct								
943 Full Attn	69.36%	73.00%	80.33%	68.00%	77.29%	63.52%	64.97%	70.92%
944 Block Attn (ICLR25)	67.92%	65.80%	68.56%	54.00%	71.75%	50.31%	61.44%	62.83%
945 APE (ICLR25)	64.22%	69.60%	65.11%	56.56%	68.70%	56.45%	58.41%	62.72%
946 Star Attn (ICML25)	58.58%	12.40%	12.89%	60.56%	51.25%	58.71%	51.90%	43.76%
947 PEVLM	69.42%	71.40%	80.11%	64.17%	76.73%	62.09%	65.08%	69.86%
948 Qwen3-VL-32B-Instruct								
949 Full Attn	74.31%	74.80%	83.00%	72.17%	77.01%	64.34%	71.03%	73.81%
950 Block Attn (ICLR25)	70.89%	68.80%	72.89%	48.17%	72.85%	41.50%	67.85%	63.28%
951 APE (ICLR25)	70.61%	72.60%	75.67%	62.94%	74.52%	53.48%	65.49%	67.90%
952 Star Attn (ICML25)	72.36%	3.60%	43.67%	59.94%	64.54%	44.16%	64.87%	50.45%
953 PEVLM	74.31%	75.60%	82.78%	68.28%	77.01%	63.63%	70.87%	73.21%

949 **(1) PEVLM is the only efficient method that closely matches Full Attention.** Across all models,
 950 the average accuracy gap between PEVLM and Full Attention is only **0.6–1.0 pp**, whereas BlockAttn,
 951 APE, and StarAttn fall behind by **8.0 pp**, **10.0 pp**, and **15.0 pp** on average, respectively. This
 952 trend holds for both Qwen3-VL family models and InternVL3_5 family models, demonstrating that
 953 PEVLM preserves the scaling benefits of larger backbones.

954 **(2) The largest gaps appear on temporal and OCR-heavy benchmarks.** In the most challenging
 955 long-range Video-MME split (2m–1h), PEVLM’s deficit to Full Attention is modest (**2.2 pp** on
 956 average), while BlockAttn and StarAttn commonly lose **10–25 pp**. Similarly, on VideoOCR, PEVLM
 957 remains within **< 1 pp** of Full Attention across all checkpoints, while APE or StarAttn are typically
 958 **4–7 pp** lower.

959 **Conclusion.** Overall, PEVLM achieves near-Full-Attention performance across all benchmarks
 960 and model scales, while other efficient attention schemes suffer substantial degradation—particularly
 961 on temporally sensitive and OCR-centric tasks. These results underscore the effectiveness and
 962 robustness of PEVLM.

972
973
974
975 Table 8: Performance (\uparrow) of InternVL3_5 models with different methods on video understanding
976 tasks evaluated at tokens from 26k to 100k.
977

Method	MVBench 17s avg.	EgoSchema 3m avg.	VideoMME < 2m	VideoMME 2m-1h	LongVideoBench < 1m	LongVideoBench 1m-1h	VideoOCR 34s avg.	Avg.
InternVL3_5-4B-Instruct								
Full Attn	69.75%	63.00%	75.00%	58.67%	71.47%	55.84%	55.33%	64.15%
Block Attn (ICLR25)	61.28%	58.60%	65.22%	52.72%	65.65%	50.31%	46.26%	57.15%
APE (ICLR25)	59.67%	61.20%	68.44%	50.39%	64.27%	48.98%	46.51%	57.07%
Star Attn (ICML25)	63.97%	61.00%	70.44%	51.61%	69.53%	51.33%	48.21%	59.44%
PEVLM	68.69%	63.40%	74.78%	58.00%	72.58%	54.92%	53.44%	63.69%
InternVL3_5-8B-Instruct								
Full Attn	70.81%	62.20%	75.89%	60.39%	72.58%	58.20%	56.31%	65.20%
Block Attn (ICLR25)	61.69%	54.80%	66.33%	53.44%	62.60%	50.61%	48.97%	56.92%
APE (ICLR25)	58.83%	60.20%	68.89%	52.28%	63.71%	51.64%	48.92%	57.78%
Star Attn (ICML25)	64.22%	61.60%	69.67%	54.11%	68.70%	54.00%	50.41%	60.39%
PEVLM	70.22%	63.60%	75.22%	59.50%	72.85%	57.99%	54.97%	64.91%
InternVL3_5-14B-Instruct								
Full Attn	70.42%	72.60%	77.22%	63.28%	74.52%	58.81%	58.87%	67.96%
Block Attn (ICLR25)	62.64%	69.00%	68.33%	55.67%	65.37%	54.61%	51.13%	60.96%
APE (ICLR25)	49.61%	68.00%	68.89%	52.28%	67.31%	53.59%	50.41%	58.58%
Star Attn (ICML25)	45.36%	70.00%	69.67%	54.11%	69.53%	53.59%	52.97%	59.32%
PEVLM	69.69%	72.80%	75.89%	63.22%	73.41%	58.40%	58.15%	67.37%
InternVL3_5-30B-A3B-Instruct								
Full Attn	75.33%	83.60%	77.67%	63.94%	74.52%	58.81%	59.33%	70.46%
Block Attn (ICLR25)	64.33%	79.60%	69.89%	58.17%	65.37%	54.61%	52.62%	63.51%
APE (ICLR25)	64.81%	79.60%	71.22%	58.11%	67.31%	53.59%	51.79%	63.78%
Star Attn (ICML25)	70.44%	79.80%	70.67%	58.89%	69.53%	53.59%	52.31%	65.03%
PEVLM	73.53%	83.00%	77.00%	62.67%	73.41%	58.40%	58.36%	69.48%

1001
1002
1003 G PER-TASK-CATEGORY ANALYSIS OF DIFFERENT PARALLEL ENCODING
1004 METHODS ON THE VIDEOMME DATASET
10051006 G.1 BENCHMARK OVERVIEW
10071008 Video-MME is a comprehensive benchmark for evaluating long-form video understanding,
1009 specifically designed to assess both perceptual and reasoning capabilities of multimodal models over
1010 extended video sequences (Fu et al., 2024). It contains a diverse set of task categories, including
1011 *Action Recognition*, *Action Perception*, *Attribute Perception*, *Information Synopsis*, *Object Reasoning*,
1012 *Counting Problem*, *Spatial & Temporal Perception*, *Spatial & Temporal Reasoning*, and *OCR-related*
1013 *Problems*. These categories jointly demand strong local perception, global integration, and long-range
1014 temporal dependency modeling. As a result, Video-MME serves as a particularly suitable benchmark
1015 for studying the effectiveness of different attention and encoding mechanisms under long-context
1016 settings.1017 In this section, we present a detailed comparison among five representative parallel encoding
1018 mechanisms: **Full Attention** (baseline), **PEVLM**, **APE**, **BlockAttn**, and **StarAttn**. The results
1019 are illustrated in radar charts on multiple model scales, including Qwen3-VL (2B, 4B, 8B, 32B) and
1020 InternVL3.5 (4B, 8B, 14B, 30B-A3B), both dense and MoE.1021
1022 G.2 OVERALL PERFORMANCE TRENDS
10231024 Across all model families and parameter scales, Full Attention generally achieves the highest accuracy,
1025 serving as an upper-bound reference with complete token-to-token interactions. However, its quadratic
complexity makes it impractical for long-context video modeling.

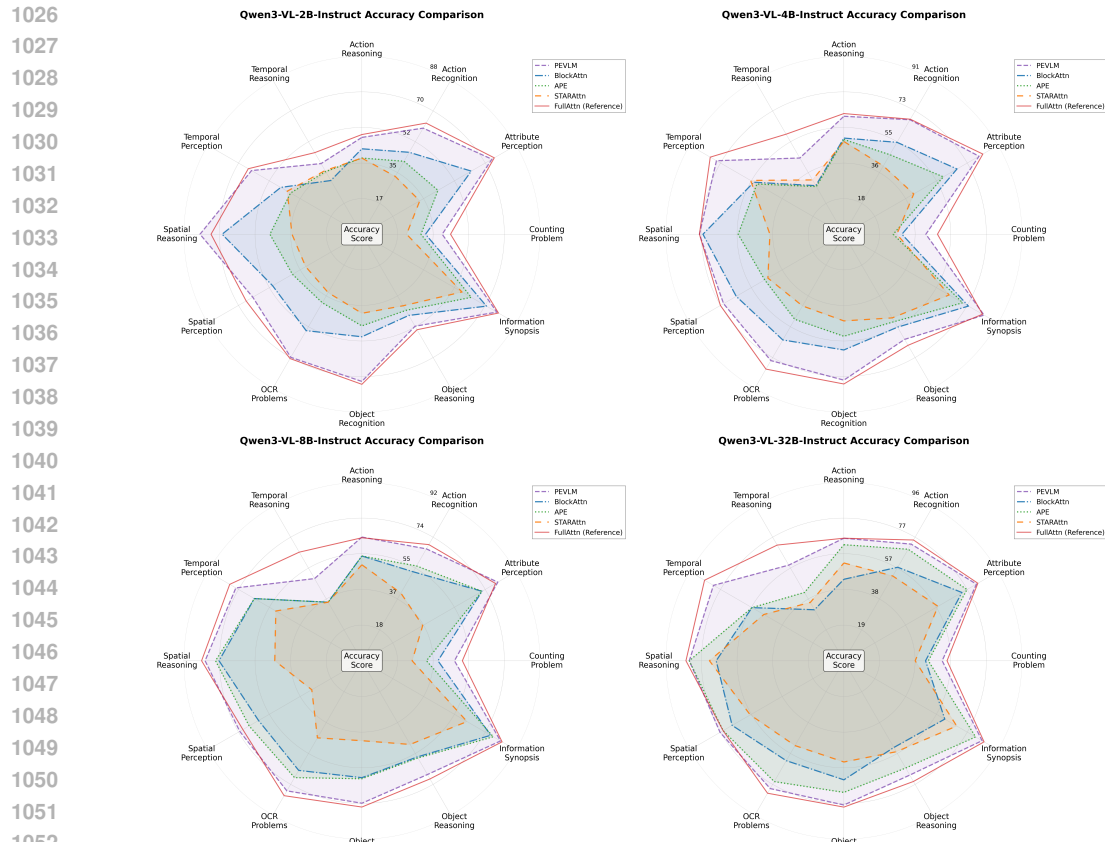


Figure 6: Radar-chart comparison of different attention mechanisms (Full Attention, PEVLM, APE, BlockAttn, StarAttn) on the Video-MME benchmark using Qwen3-VL models. PEVLM achieves consistently higher accuracy across temporally sensitive and spatially fine-grained tasks, while methods that reuse position embeddings (APE, BlockAttn, StarAttn) exhibit noticeable degradation in temporal-related and OCR-related categories.

Among the efficient alternatives, **PEVLM consistently demonstrates the closest performance to Full Attention** in almost all task categories and model scales. In contrast, both **APE** and **StarAttn** exhibit considerable performance degradation in perception-intensive and reasoning-heavy tasks, while **BlockAttn** shows moderate but unstable performance across different categories.

Notably, the relative advantage of PEVLM becomes increasingly pronounced as the model scale grows (e.g., Qwen3-VL-32B and InternVL3.5-14B/30B), suggesting that PEVLM better preserves the benefits of larger backbone models under long-sequence constraints.

1069 G.3 CATEGORY-WISE ANALYSIS

1071 **Information Synopsis and Object Reasoning.** These two categories demonstrate the most
 1072 significant and consistent advantages for PEVLM over other efficient methods. Both tasks require the
 1073 integration of long-range semantic information across distant frames. Block-based or sparse attention
 1074 structures, such as in BlockAttn and StarAttn, tend to fragment the video representation, leading
 1075 to incomplete global understanding. In contrast, PEVLM’s parallel encoding strategy preserves
 1076 high-level temporal coherence, enabling superior global summarization and reasoning performance.

1078 **Attribute Perception and Action Recognition.** PEVLM also closely matches Full Attention on
 1079 fine-grained perceptual tasks. This indicates that its sink+divide strategy does not overly sacrifice
 local pixel-level or frame-level discriminative features. APE, on the other hand, shows noticeable

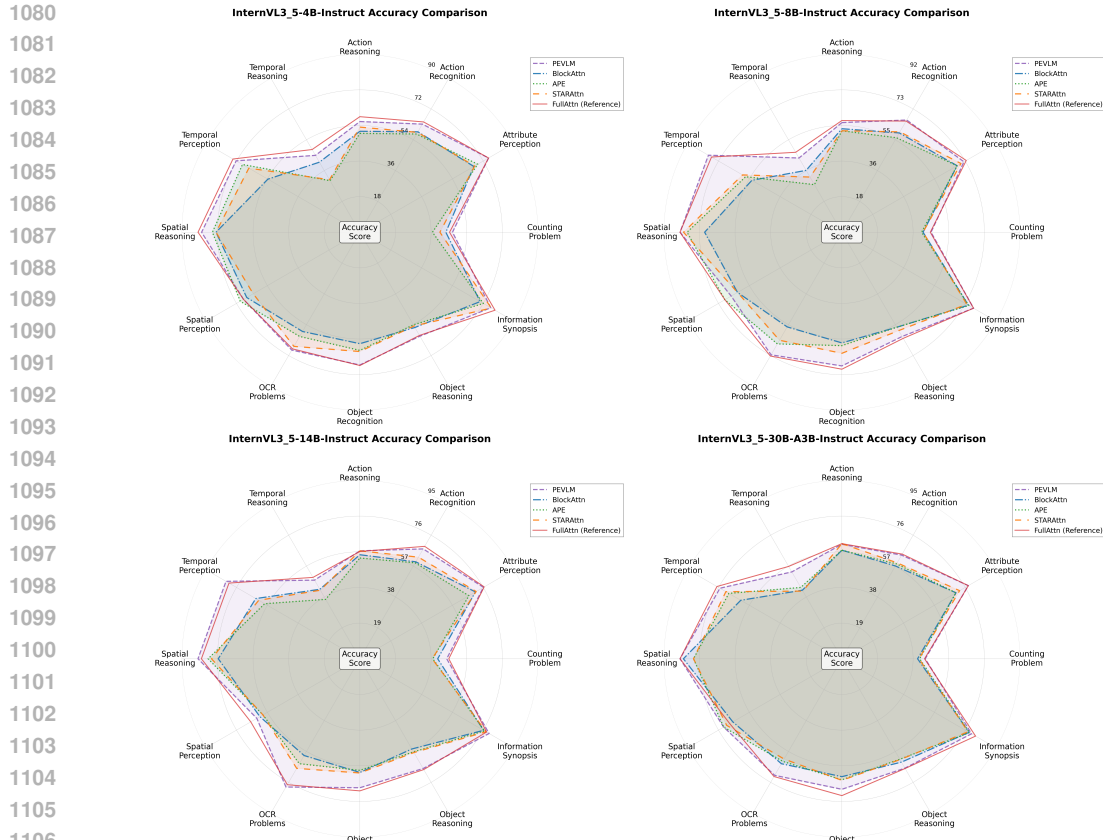


Figure 7: Radar-chart comparison of attention mechanisms on the Video-MME benchmark using InternVL3.5 models. Similar to Qwen3-VL results, PEVLM remains close to Full Attention and outperforms other parallel encoding baselines, particularly on tasks requiring strict temporal ordering and stable cross-frame alignment.

degradation in these tasks, likely due to its sensitivity to hyperparameters and unstable alignment with the original attention score distribution.

Temporal Reasoning and Temporal Perception. These categories highlight the difficulty of modeling long-term motion patterns and temporal dependencies. StarAttn and BlockAttn struggle to maintain cross-block temporal consistency, resulting in lower scores. In comparison, PEVLM maintains a smoother performance profile, indicating that its design better captures temporal continuity without incurring the full cost of quadratic attention.

Spatial Reasoning and OCR Problems. Although all efficient methods show some performance drop relative to Full Attention, PEVLM consistently ranks first among them. OCR and spatial tasks depend on both fine spatial features and long-range context (e.g., multi-frame text aggregation), which PEVLM’s frame-aware parallel representation can retain more effectively.

G.4 SCALABILITY ACROSS MODEL SIZES

A critical observation from the radar plots is that PEVLM scales more favorably with increasing backbone capacity. While the relative gap between Full Attention and other methods slightly widens for APE and StarAttn at larger model sizes, PEVLM continues to closely track the Full Attention curve.

1134 This indicates that PEVLM does not bottleneck the expressive power of larger VLMs. Instead, it
 1135 allows the model to effectively leverage additional parameters even under parallel encoding constraints.
 1136 Such scalability is essential for future high-capacity VLMs targeting long-video understanding.
 1137

1138 **G.5 KEY ADVANTAGES OF PEVLM**

1140 From both empirical and architectural perspectives, PEVLM exhibits three major advantages:

1141

- 1142 • **High Fidelity to Full Attention:** PEVLM consistently achieves the closest approximation
 1143 to Full Attention across almost every task and model size.
- 1144 • **Robustness Across Categories:** Unlike APE and BlockAttn, whose performance fluctuates
 1145 significantly by task type, PEVLM maintains stable superiority across both perceptual and
 1146 reasoning-based categories.
- 1147 • **Scalable and Training-Free:** PEVLM requires no fine-tuning or architectural modification,
 1148 making it highly practical for deployment in existing VLM pipelines while still benefiting
 1149 from scaling laws.

1150 These results validate that PEVLM provides an effective and efficient alternative to Full Attention
 1151 for long-context video understanding, striking an optimal balance between accuracy, scalability, and
 1152 computational cost.

1153
 1154
 1155
 1156
 1157
 1158
 1159
 1160
 1161
 1162
 1163
 1164
 1165
 1166
 1167
 1168
 1169
 1170
 1171
 1172
 1173
 1174
 1175
 1176
 1177
 1178
 1179
 1180
 1181
 1182
 1183
 1184
 1185
 1186
 1187

H ATTENTION SCORES DISTRIBUTION OF LLAVA-VIDEO AND LONGVILA

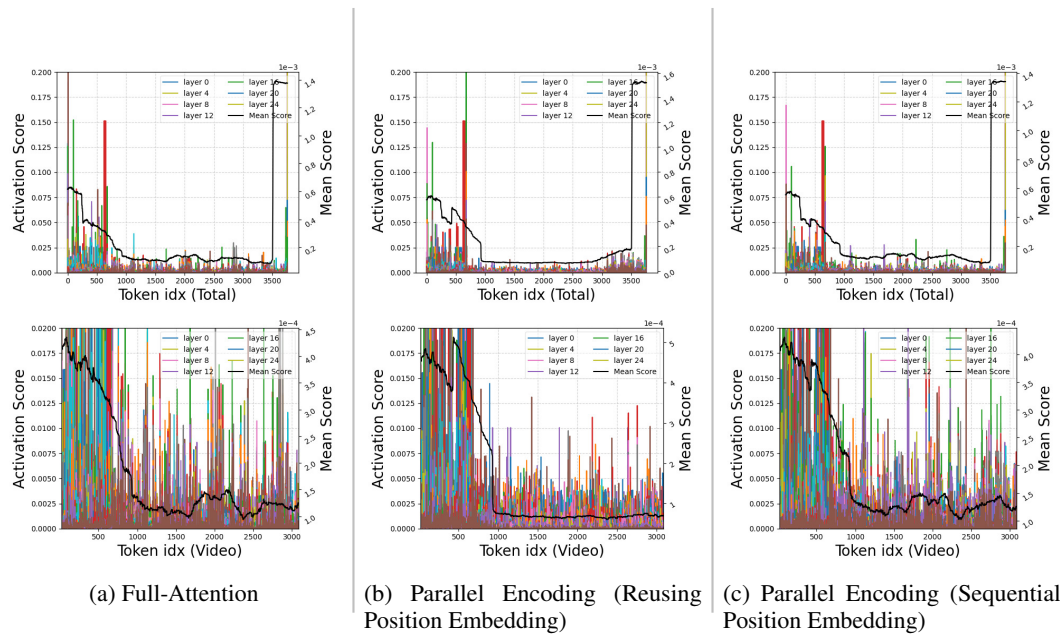


Figure 8: Attention Scores Distributions of Qwen2.5-VL. The top row shows the attention scores for all tokens, while the bottom row shows those for the visual tokens.

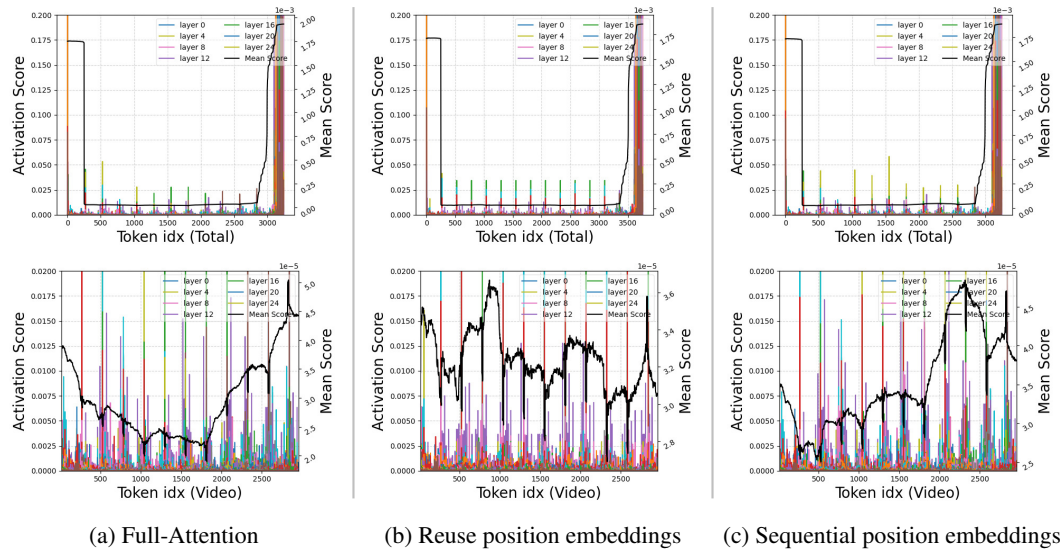


Figure 9: Attention Scores Distributions of LongVILA. The top row shows the attention scores for all tokens, while the bottom row shows those for the visual tokens.

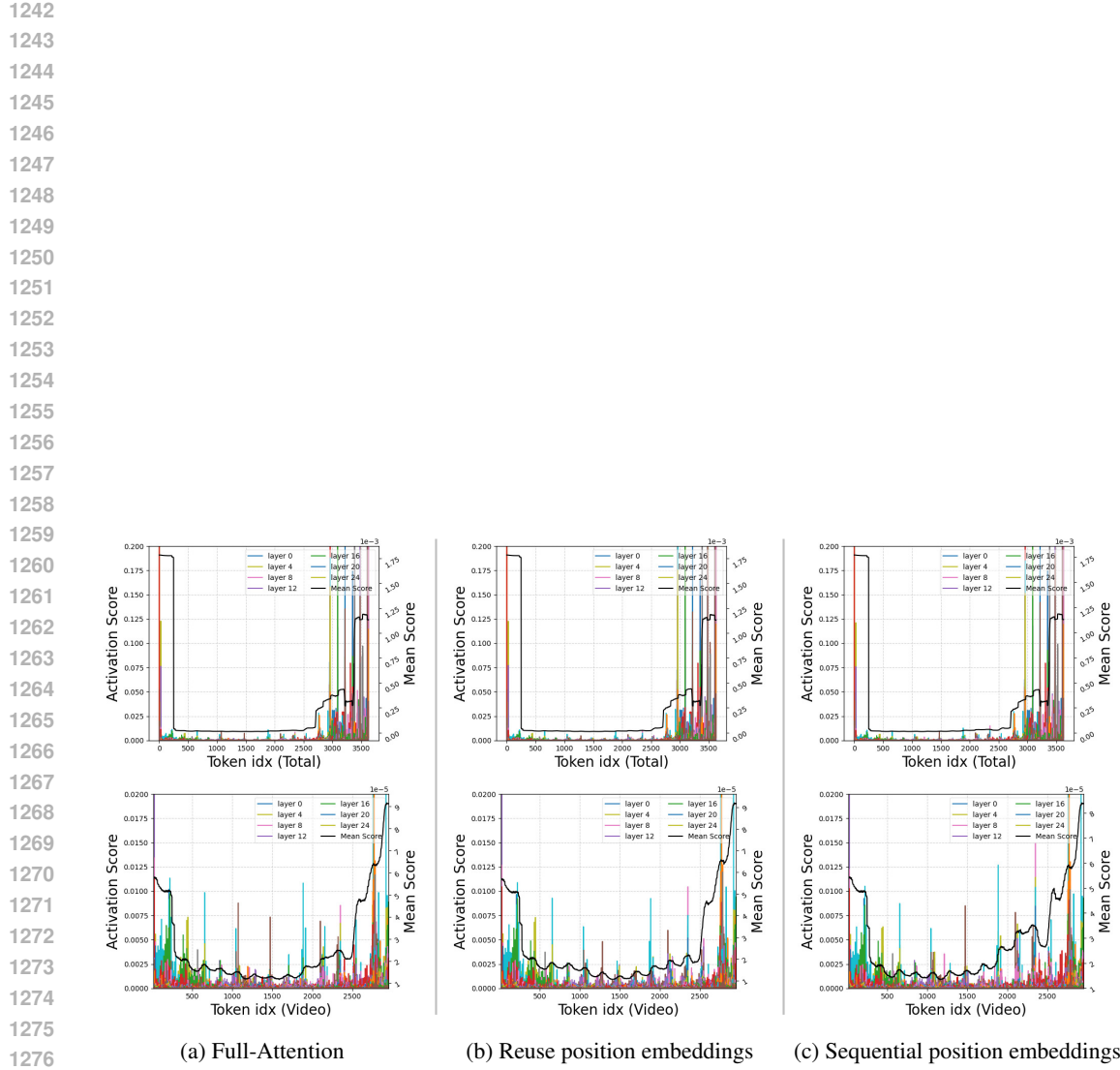


Figure 10: Attention Scores Distributions of LLaVA-Video. The top row shows the attention scores for all tokens, while the bottom row shows those for the visual tokens.